npg

Original Article

Apogossypolone, a novel inhibitor of antiapoptotic Bcl-2 family proteins, induces autophagy of PC-3 and LNCaP prostate cancer cells *in vitro*

Xian-Qing Zhang[1, *], Xiao-Feng Huang[2, *], Xing-Bin Hu[1], Yong-Hua Zhan[3], Qun-Xing An[1], Shi-Ming Yang[4], Ai-Jun Xia[1], Jing Yi[1], Rui Chen[1], Shi-Jie Mu[1], Dao-Cheng Wu[5]

[1]*Department of Blood Transfusion, Xijing Hospital, Fourth Military Medical University, Xi'an 710032, China*
[2]*Central Laboratory, School of Basic Medicine, Fourth Military Medical University, Xi'an 710032, China*
[3]*School of Life Sciences and Technology, Xidian University, Xi'an 710071, China*
[4]*Department of Blood Transfusion, Tangdu Hospital, Fourth Military Medical University, Xi'an 710038, China*
[5]*The Key Laboratory of Biomedical Information Engineering of the Ministry of Education, Xi'an Jiaotong University, Xi'an 710038, China*

Abstract

Limited treatment options are available for aggressive prostate cancer. Gossypol has been reported to have a potent anticancer activity in many types of cancer. It can increase the sensitivity of cancer cells to alkylating agents, diminish multidrug resistance and decrease metastasis. Whether or not it can induce autophagy in cancer cells has not yet been determined. Here we investigated the antiproliferative activity of apogossypolone (ApoG2) and (−)-gossypol on the human prostate cancer cell line PC3 and LNCaP *in vitro*. Exposure of PC-3 and LNCaP cells to ApoG2 resulted in several specific features characteristic of autophagy, including the appearance of membranous vacuoles in the cytoplasm and formation of acidic vesicular organelles. Expression of autophagy-associated LC3-II and beclin-1 increased in both cell lines after treatment. Inhibition of autophagy with 3-methyladenine promoted apoptosis of both cell types. Taken together, these data demonstrated that induction of autophagy could represent a defense mechanism against apoptosis in human prostate cancer cells.

Correspondence to: Prof. Dao-Cheng Wu, The Key Laboratory of Biomedical Information Engineering of Ministry of Education, Xi'an Jiaotong University, 28 West Xianning Road, Xi'an 710038, China.
Fax:+86-29-8266-3941   E-mail: wudaocheng@mail.xjtu.edu.cn
and Prof. Shi-Jie Mu, Department of Blood Transfusion, Xijing Hospital, Fourth Military Medical University, Xi'an 710032, China.
Fax: +86-29-8324-4952   E-mail: sxkhla@mail.xjtu.edu.cn
*These authors contributed equally to this work.

1 Introduction

Cells encountering a variety of stresses undergo an evolutionarily conserved process of self-digestion termed autophagy. The importance of this intracellular damage response has been established in infectious diseases, neurodegeneration, heart failure and cancer [1]. In cancer, the debate continues as to whether or not autophagy is primarily a mechanism of cell death or cell survival. This is important to answer in order to promote the clinical development of therapeutic

interventions that can either inhibit or enhance autophagy in tumor cells. A number of clinically available cancer therapeutics, including DNA damaging chemotherapy, radiation therapy and molecularly targeted therapies, have been found to induce autophagy in cell culture and animal models [2].

Autophagy has two conflicting functions in cell biology. It has been shown that hepatocellular carcinoma down-regulates autophagic activity [3, 4], but recently, autophagy has been proposed as a tumor suppression mechanism, underlying the possibility that activation of autophagy reverses the neoplastic phenotype [5]. Cancer cells can respond to drugs by activating autophagy to promote cell survival, thus counteracting apoptosis [6]. Inhibition of autophagy would likely enhance apoptosis, indicating that autophagy contributes to tumor progression as a protective mechanism against stressful conditions [7, 8]. Longo *et al.* [9] reported that autophagy inhibition helped to enhance the chemopreventive/therapeutic activity of anthocyanin against hepatocellular carcinoma.

Prostate cancer is the most common malignancy and the second leading cause of cancer mortality in men. Unfortunately, there are limited treatment options available for this disease once primary therapies fail [10, 11]. Furthermore, an earlier diagnosis, which is necessary for surgery or irradiation is difficult to achieve [12]. Thus, newer therapies are badly needed.

The natural polyphenolic compound, gossypol, a promising male contraceptive drug candidate [13, 14], has been reported to have potent anticancer activities [15, 16]. It has been shown to increase the sensitivity of cancer cells to alkylating agents [17]. Gossypol was also reported to be effective in treating multidrug-resistant cancer [18]. Furthermore, gossypol could decrease the metastasis of adrenal carcinoma, glioma and breast carcinoma [19]. Gossypol inhibits proliferation of MAT-LyLu Dunning prostate cancer cells *in vitro*, and also inhibits metastasis in xenografts [20]. In addition, gossypol inhibits proliferation or induces apoptosis of PC-3 human prostate cancer cells *in vitro* [20, 21]. (–)-Gossypol, the (–)-enantiomer of gossypol, also inhibits tumor growth in PC-3 xenografts, and sensitizes the anticancer effect of radiation therapy [21].

It has been shown that gossypol induces apoptosis in PC-3 cells by modulating caspase-dependent and caspase-independent cell death pathways [22]. Apogossypolone (ApoG2) is a semi-synthesized derivative of gossypol that binds to the Bcl-2 family proteins in the low nanomolar range with a K_i of 35 and 25 nmol L^{-1} for Bcl-2 and Mcl-1, respectively, and a K_i of 660 nmol L^{-1} for Bcl-XL [23]. It has been proven that ApoG2 can be an effective therapeutic agent against follicular lymphoma by inducing apoptosis in a preclinical study [23]. ApoG2 has higher antitumor activity and lower toxicity than gossypol [24]. Whether or not it can induce autophagy in PC-3 and LNCaP prostate cancer cells remains unclear. The present study shows a novel response in PC-3 and LNCaP cells to ApoG2 involving the formation of acidic vesicular organelles (AVOs) and autophagy.

2 Materials and methods

2.1 Cell culture

PC-3 and LNCaP cells were purchased from the American Type Culture Collection (ATCC, Manassas, VA, USA). PC-3 cells were cultured in RPMI-1640 media (Gibco BRL, Grand Island, NY, USA) supplemented with 100 IU mL^{-1} penicillin G sodium, 100 mg mL^{-1} streptomycin sulfate and 10% (v/v) fetal bovine serum (Hyclone Laboratories, Logan, UT, USA). LNCaP cells were cultured in RPMI 1640 supplemented with 10% fetal bovine serum, 10 mmol L^{-1} HEPES, 1 mmol L^{-1} sodium pyruvate, 0.2% (w/v) glucose and antibiotics. Each cell line was maintained at 37ºC in a humidified incubator with 5% CO_2.

2.2 Preparation of ApoG2 and (−)-gossypol

ApoG2 was synthesized by the College of Life Science and Technology of Xi'an Jiaotong University (Xi'an, China). Its purity was determined by high-pressure liquid chromatography analysis, showing a chemical purity of > 99%. (−)-Gossypol was purified at the College of Life Science and Technology of Xi'an Jiaotong University. Its chemical purity was > 98% with a chiral purity of > 97%. Stock solutions of 100 mg mL^{-1} ApoG2 and (–)-gossypol were prepared by dissolving ApoG2 or (–)-gossypol in 100% (v/v) dimethyl sulfoxide (DMSO) on the day of use. Working solutions were obtained by dilution of the stock solutions with culture medium.

2.3 MTT assay for cell growth and viability

Cell growth and viability were evaluated using the MTT assay (Sigma-Aldrich, St. Louis, MO, USA) [25]. PC-3 or LNCaP cells harvested from routine cultures were suspended in media and plated into 96-well microtiter plates at a density of 5×10^5 per well in a volume of 0.1 mL. After plating and incubation of the

cells for 24 h, serially diluted ApoG2 or (−)-gossypol-containing media were added to the wells at a volume of 0.1 mL per well to give a final concentration of 5, 10 and 20 mg L^{-1}. To determine the effect of 3-methyladenine (3-MA) on the growth of prostate cancer cells, the survival rate of PC-3 and LNCaP cells was measured in the presence and absence of 10 mmol L^{-1} 3-MA. After exposure to the test drugs at 37ºC for 24, 48, 72 or 96 h, the cells were incubated with MTT for 4 h; the plates were processed and the absorbance (optical density) was detected as described by Romijn *et al.* [25]. Eight replicates were done for each experimental condition. The percentage of surviving cells was defined as mean absorbance of treated wells/mean absorbance of untreated wells.

2.4 Autophagy detection with acridine orange staining

As a marker of autophagy, the volume of the cellular acidic compartment was visualized by acridine orange (Molecular Probes, Eugene, OR, USA) staining [26]. In acridine orange-stained cells, the cytoplasm and nuclei fluoresce bright green and dim red, respectively, whereas the acidic compartment fluoresces bright red [27, 28]. The intensity of red fluorescence is proportional to the degree of acidity. Therefore, the volume of the cellular acidic compartment can be quantified [26, 27]. Cells were seeded in 96-well plates and treated as described above. At the various time points following treatment, cells were incubated with 1 mg L^{-1} acridine orange for 15 min. The dye was removed and fluorescence micrographs were taken using an inverted microscope equipped with a 100-W mercury lamp, 490-nm band-pass blue excitation filters, a 500-nm dichroic mirror and a 515-nm long-pass barrier filter. Autophage was quantified based on the mean number of cells displaying intense red staining in three fields (containing at least 50 cells per field) for each experiment condition.

2.5 Immunocytochemistry

PC-3 or LNCaP cells (10^5) were grown on coverslips and allowed to attach by overnight incubation. The cells were then exposed to DMSO or 5, 10 and 20 mg L^{-1} ApoG2 or (−)-gossypol for the time periods mentioned above at 37ºC, washed with PBS and fixed at 4ºC overnight using 4% (w/v) paraformaldehyde. Subsequently, the cells were washed with PBS, and blocked with PBS containing 0.5% (w/v) bovine serum albumin (BSA) and 0.15% (w/v) glycine (BSA buffer) for 1 h at room temperature (RT). Cells were treated with rabbit anti-LC3-II (Abcam,

Cambridge, UK) at 1:100 dilution in BSA buffer or rabbit anti-beclin-1 (Abcam) at 1:400 dilution in BSA buffer) for 1 h at RT. Cells were then washed with BSA buffer and incubated with FITC-conjugated goat anti-rabbit (Abcam) at 1:100 dilution in BSA buffer for 1 h at RT. Slides were mounted and examined under a fluorescence microscope (Olympus, Tokyo, Japan). Microtubule-associated protein 1A/1B-light chain 3 (LC3) is a soluble protein with a molecular mass of approximately 17 kDa distributed ubiquitously in mammalian tissues and cultured cells. During autophagy, autophagosomes engulf cytoplasmic components, including cytosolic proteins and organelles. Concomitantly, a cytosolic form of LC3 (LC3-I) is conjugated to phosphatidylethanolamine to form LC3-phosphatidylethanolamine conjugate (LC3-II), which is recruited to autophagosomal membranes. Autophagosomes fuse with lysosomes to form autolysosomes, and intra-autophagosomal components are degraded by lysosomal hydrolases. At the same time, LC3-II in the autolysosomal lumen is degraded. Thus, lysosomal turnover of the autophagosomal marker LC3-II reflects autophagic activity, and detecting LC3-II by immunofluorescence has become a reliable method for monitoring autophagy and autophagy-related processes. Beclin-1 was identified in a yeast two-hybrid screen as a Bcl-2-interacting protein [29]. It has a key role in autophagy [30–34], regulates the autophagy-promoting activity of Vps34 [35], and is involved in the formation of autophagosomes. Beclin 1 also interacts with Bcl-2, and may thus be involved in regulating cell death [29]. Luo and Rubinsztein [36] have proved that apoptosis induced by the proapoptotic protein Bax inhibited autophagy by enhancing caspase-mediated cleavage of Beclin-1. After cleavage, Beclin-1 does not interact with Vps34. It was shown that Bcl-2 binds to Beclin-1 to disrupt its autophagy function [37].

2.6 Ultrastructure of treated PC-3 and LNCaP cells

Transmission electron microscopy (JEOL, Tokyo, Japan) was used to examine the effect of ApoG2 or (−)-gossypol treatment on PC-3 and LNCaP cells as described previously [38]. Briefly, PC-3 or LNCaP cells (2 × 10^5) were plated in six-well plates overnight, and were then treated with either DMSO (control) or 5, 10 and 20 mg L^{-1} ApoG2 or (−)-gossypol for 24, 48, 72 or 96 h at 37ºC. The cells were harvested by trypsinization, washed twice with PBS and fixed in 2.5% (w/v) ice-cold electron microscopy-grade glutaraldehyde in PBS (pH 7.3). The specimens were rinsed with PBS, postfixed in 1% (w/v) osmium

tetroxide, dehydrated through a graded series of ethanol (30%–90%) and embedded in Epon 812 resin. Ultrathin 100-nm sections were cut using a LKB NOVA ultramicrotome (LKB-NOVA, Bromma, Sweden), stained with 2% (w/v) uranyl acetate and lead citrate, and examined on a JEM-2000EX transmission electron microscope (JEOL) at either $\times$ 4 000 or $\times$ 8 000 magnification.

2.7 Detection of apoptosis and autophagy by flow cytometry

The percentage of autophagic cell death was analyzed using flow cytometry with acridine orange staining according to published procedures [24]. Cells (2×10^5) were treated with either DMSO or 5, 10 and 20 mg L^{-1} ApoG2 or (–)-gossypol for 48 h at 37ºC. The cells were then stained with acridine orange (1 g L^{-1}) for 20 min. The trypsinized adhered cells and the suspended cells in medium were collected in phenol red-free RPMI 1640 medium. The green (510–530 nm) and red (650 nm) fluorescence emission from 1×10^4 cells were measured with a flow cytometer using CellQuest software. The percentage of autophagy was calculated from the events recorded in the upper-left and upper-right quadrants of the flow cytograms. 3-MA was used to detect its effect on 10 mg L^{-1} ApoG2-treated cells. The cells were treated with 10 mmol L^{-1} 3-MA and 10 mg L^{-1} ApoG2 for 48 h and the percentage of autophagic cell death was analyzed as above. Apoptosis was analyzed by detecting phosphatidylserine (PS) externalization using flow cytometry with two-color analysis of FITC-labeled Annexin V/propidium iodide (PI) double staining [28, 39]. In brief, PC-3 or LNCaP cells (2×10^5) were treated with either DMSO or 5, 10 and 20 mg L^{-1} ApoG2 or (–)-gossypol for 24, 48, 72 or 96 h at 37ºC. The cells were trypsinized, washed in cold PBS, stained with 1 mg L^{-1} FITC-labeled Annexin V and 0.2 mg L^{-1} PI (Sigma-Aldrich) for 15 min, and analyzed by flow cytometry (FACSAria, Becton Dickinson, Mountainview, CA, USA). Measure of apoptosis was scored from primary apoptosis (Annexin V$^+$/PI$^-$) and late apoptosis (Annexin V$^+$/PI$^+$) events.

2.8 TUNEL assay

The method of Gavrieli *et al.* [40] was utilized as an independent assessment of apoptotic cell death. Adherent cells treated with 10 mg L^{-1} ApoG2 or (–)-gossypol were fixed and cells undergoing apoptosis were detected using the *in situ* cell death detection kit (Boehringer-Mannheim, Mannheim, Germany). For the apoptotic effects of 3-MA, 10 mmol L^{-1} 3-MA was added to the culture before 10 mg L^{-1} ApoG2. The TUNEL assay was performed according to the manufacturer's instructions. Cells were then washed, mounted in vectashield mounting medium with Hoechst 33342 (Sigma-Aldrich) and photographed using the FV1000 laser scanning confocal microscope (Olympus). A positive control was prepared by treating a sample with DNaseI before TUNEL staining. For quantitative analysis, the percentage of TUNEL-positive cells among 200 cells in three fields per section was determined at $\times$ 200 magnification.

2.9 Statistical analysis

SPSS version 11.0 (SPSS Inc., Chicago, IL, USA) was used for all statistical analyses. All data were presented as mean $\pm$ SD. Statistical analysis was performed using the unpaired *t*-test. $P < 0.05$ was considered as statistically significant.

3 Results

3.1 ApoG2 and (−)-gossypol inhibited PC-3 and LNCaP cell growth

As shown in Figure 1A, (–)-gossypol inhibited PC-3 cell growth in a dose-dependent manner. In all, 20 mg L^{-1} (−)-gossypol showed the most significant growth inhibition on PC-3 cells, and the cell survival ratio was only 12% at 96 h. Similar growth inhibition of (−)-gossypol on LNCaP cells was observed. More than 85% LNCaP cells were lysed after 20 mg L^{-1} (−)-gossypol was administered for 96 h (Figure 1B). The inhibitory effect of ApoG2 on PC-3 and LNCaP cells was similar to that of (–)-gossypol and the dose-dependent effect was also evident (Figures 1C and D). The viability of cells treated with 3-MA also decreased in both cell lines, but just slightly (Figure 1). When both cell lines were treated with 3-MA and ApoG2, an enhanced growth inhibitory effect was observed (Figure 1).

3.2 (−)-Gossypol and ApoG2 induced apoptosis and autophagy in PC-3 and LNCaP

Translocation of PS from the internal side of the plasma membrane to the external occurs in the early stages of apoptosis. Annexin V is a Ca^{2+}-dependent phospholipid-binding protein with high affinity for PS, and can be used as a sensitive probe for apoptosis. PS translocation is not unique to apoptosis and occurs

Apogossypolone induces autophagy of prostate cancer cells *in vitro*
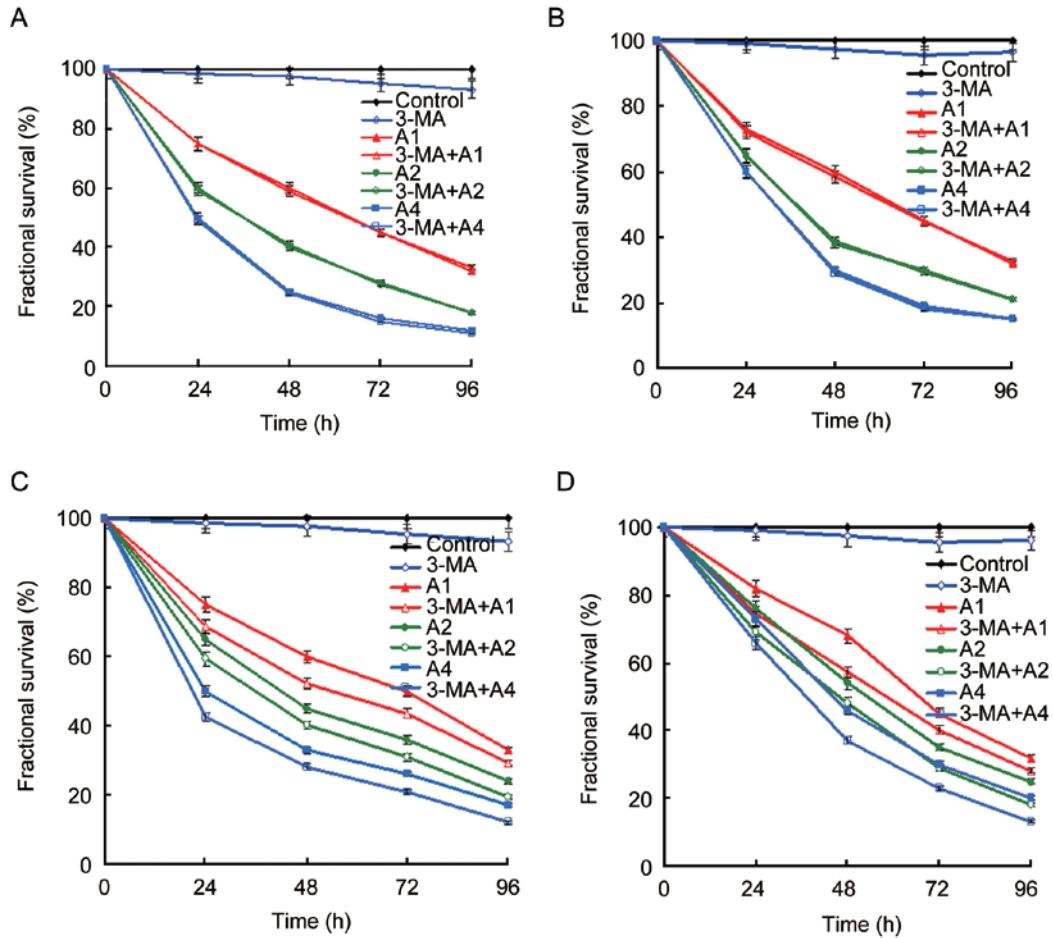Xian-Qing Zhang *et al*.

npg

701

Figure 1. Time- and dose-dependent growth inhibition by (–)-gossypol (A, B) and ApoG2 (C, D) in PC-3 cells (A, C) and LNCaP cells (B, D). PC-3 or LNCaP cells were treated with different concentrations of (–)-gossypol or ApoG2 for various times. The experimental groups are as follows: control, cells treated with DMSO; 3-MA, cells treated with 10 mmol L^{-1} 3-MA; A1, cells treated with 5 mg L^{-1} (–)-gossypol or ApoG2; 3-MA + A1, cells treated with 10 mmol L^{-1} 3-MA + 5 mg L^{-1} (–)-gossypol or ApoG2; A2, cells treated with 10 mg L^{-1} (–)-gossypol or ApoG2; 3-MA + A2, cells treated with 10 mmol L^{-1} 3-MA + 10 mg L^{-1} (–)-gossypol or ApoG2; A4, cells treated with 20 mg L^{-1} (–)-gossypol or ApoG2; 3-MA + A4, cells treated with 10 mmol L^{-1} 3-MA + 20 mg L^{-1} (–)-gossypol or ApoG2.

also in necrosis. The difference between these two forms of cell death is that during the initial stages of apoptosis the cell membrane remains intact, while at the time of necrosis the cell membrane loses its integrity. Therefore, Annexin V binding as indicative of apoptosis has to be measured in conjunction with a dye exclusion test to assess cell membrane integrity. In the flow analysis data plots, the lower left quadrant shows viable cells, which exclude PI and are negative for FITC-Annexin V binding (Annexin V^-/PI^-). The upper right quadrant shows non-viable, necrotic cells or late apoptotic cells, positive for FITC-Annexin V binding and PI uptake (Annexin V^+/PI^+). The lower

right quadrant shows early or primary apoptotic cells and Annexin V^+/PI^-. Since late apoptotic and necrotic cells cannot be distinguished, the percentage of apoptosis was scored from the Annexin V^+/PI^- and Annexin V^+/PI^+ events.

As shown in Figures 2A and B, exposure to 20 mg L^{-1} of (–)-gossypol led to apoptosis in more than 45.7% of PC-3 cells and 42.1% of LNCaP cells. In contrast, the percentage of apoptosis was 14.3% of PC-3 cells when exposed to 20 mg L^{-1} ApoG2 (Figure 2C), and 10.8% of LNCaP cells (Figure 2D). These data indicated that unlike (–)-gossypol, ApoG-2 induced apoptosis to a lesser extent.

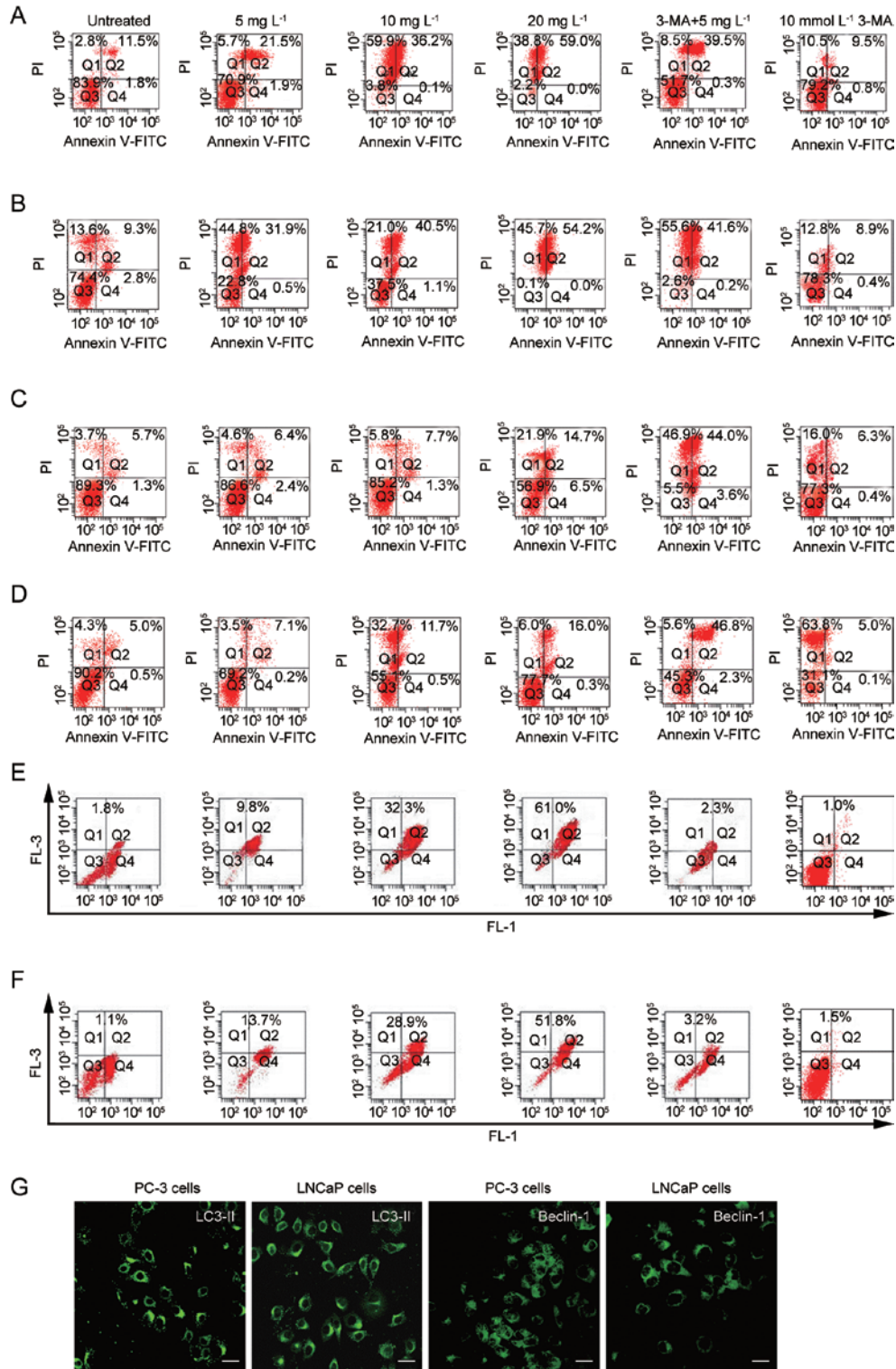When 3-MA was administered with ApoG2, the

Figure 2. Apoptosis and autophagy are induced by ApoG2 or (−)-gossypol in PC-3 and LNCaP cells. PC-3 cells (A) or LNCaP (B) cells treatment with different concentrations of (−)-gossypol for 48 h and apoptosis was detected by flow cytometry; PC-3 cells (C) or LNCaP cells (D) treatment with different concentrations of ApoG2 for 48 h and apoptosis was detected by flow cytometry; PC-3 cells (E) or LNCaP cells (F) treatment with different concentrations of ApoG2 for 48 h and autophagy was analyzed using flow cytometry with acridine orange staining. (G): Expression of LC-3-II and Beclin-1 in PC-3 and LNCaP cells. PC-3 or LNCaP cells treated with 10 mg L^{-1} ApoG2 for 48 h. Bars = 20 μm.

Apogossypolone induces autophagy of prostate cancer cells *in vitro*
Xian-Qing Zhang *et al*.

npg

703

percentage of apoptosis was increased from 2.0% to 40.6% in PC-3 cells, and from 6.7% to 43.6% in LNCaP cells (Figures 2C and D). Co-treatment with 3-MA and 10 mg L^{-1} (−)-gossypol showed little effect on apoptosis (Figure 2A and 2B). There was no significant effect on apoptosis by 3-MA alone (Figure 2). These results indicated that autophagy inhibition may serve to render cells susceptible to ApoG2-induced cell death.

AVOs and LC3-II were used to examine drug-treated PC-3 and LNCaP cells. As shown in Figures 2E and F, the percentage of AVO-positive cells increased to 61.0% in PC-3 cells and to 51.8% in LNCaP cells at a concentration of 20 mg L^{-1} ApoG2. No significant difference in the ratio of AVO was found between control and cells treated with 3-MA (Figure 2). Immunohistochemical results showed that the DMSO-treated PC-3 or LNCaP cells exhibited little LC3-II signal (data not shown). On the other hand, PC-3 cells treated for 48 h with 10 mg L^{-1} ApoG2 displayed a punctate pattern for LC3-II and beclin-1 staininge, which characterizes their redistribution to autophagosomes (Figure 2G). No obvious LC3-II or beclin-1 signals were found in (−)-gossypol-treated PC-3 or LNCaP cells (data not shown). When 3-MA was combined with 10 mg L^{-1} ApoG2, the ratio of AVO decreased from 32.3% to 2.3% in PC-3 cells and from 28.9% to 3.2% in LNCaP cells (Figures 2E and F). No significant difference in the ratio of AVO was found between control and 3-MA (Figure 2). Here, increased levels of the autophagosomal marker LC3-II was detected by immunofluorescence after ApoG2 treatment, indicating the presence of autolysosomes or autophagolysosomes [41].

3.3 Morphology of apoptosis and autophagy induced by (−)-gossypol and ApoG2 in PC-3 and LNCaP cells

As shown in Figures 3A–J, the upper pannels consisted of PC-3 cells and the lower pannels LNCaP cells. Upon treatment with 10 mg L^{-1} ApoG2, PC-3 (Figure 3B) or LNCaP (Figure 3G) cells showed negligible amounts of TUNEL-positive nuclei when compared with controls (Figures 3A and 3F), whereas PC-3 (Figure 3C) cells or LNCaP (Figure 3H) cells treated with 10 mg L^{-1} (−)-gossypol showed an increase of TUNEL-positive nuclei. When 10 mg L^{-1} ApoG2 plus 10 mmol L^{-1} 3-MA was used, TUNEL-positive nuclei were obviously increased (Figures 3D and I). The number of TUNEL-positive nuclei in cells treated with 3-MA alone was similar to that of the DMSO group (Figures 3E and J). Cell counts were made

according to the staining pattern (Figure 3K). The control group of PC-3 cells showed less apoptotic cell death than the ApoG2 group (1.2% ± 0.1% *vs.* 3.2% ± 0.3%), but the difference was not significant ($P > 0.05$). (−)-Gossypol induced significant increases in apoptotic cell death relative to control ($P < 0.01$). Results from LNCaP cells were similar. When 3-MA was added, the percentage of apoptotic cells induced by ApoG2 increased to 42.1% in PC-3 cells and to 45.6% in LNCaP cells, and this increase was significant ($P < 0.01$, Figure 3K).

Electron microscopy was used to reveal the formation of autophagosomes in ApoG2-treated PC-3 cells. As shown in Figure 4A, DMSO-treated PC-3 cells exhibited large nuclei with prominent nucleoli, and uniform and finely dispersed chromatin. No autophagic vacuoles were observed, and microvilli were preserved on the cell surface. PC-3 cells treated for 24 h with 10 mg L^{-1} ApoG2 showed large vacuoles in the cytoplasm. Nuclei of these cells appeared normal with no sign of chromatin condensation. Formation of these vacuoles increased progressively with increasing ApoG2 exposure time. Some of the vacuoles resembled autophagosomes and contained remnants of degraded organelles (Figure 4B). At 72 h, microvilli were missing, the cytoplasm was filled with vacuoles, and the nuclei displayed chromatin condensation, characteristic of cells undergoing apoptosis (Figure 4C).

The ultrastructure of PC-3 cells treated with DMSO for 72 h appeared normal (Figure 4D). That of PC-3 cells treated for 24 h with 10 mg L^{-1} (−)-gossypol revealed no autophagic vacuoles. There was no microvilli swelling, and the nuclei showed chromatin condensation and DNA fragmentation (Figure 4E). The number of these cells increased progressively with increasing (−)-gossypol exposure. These results indicated that ApoG2 treatment caused formation of autophagosome-like structures, and that this cellular response occurred before the onset of apoptosis.

The effect of ApoG2 treatment on AVO formation in PC-3 cells was determined by fluorescence microscopy and acridine orange staining [42]. As shown in Figure 5A, DMSO-treated PC-3 cells primarily exhibited green fluorescence, indicating a lack of AVO. On the other hand, treatment of PC-3 cells with 10 mg L^{-1} ApoG2 for 24 h (Figure 5B) or 96 h (Figure 5C) resulted in formation of AVO indicated by red fluorescence, which increased with exposure. PC-3 cells treated with 10 mg L^{-1} (−)-gossypol for 72 h appeared primarily green with rare
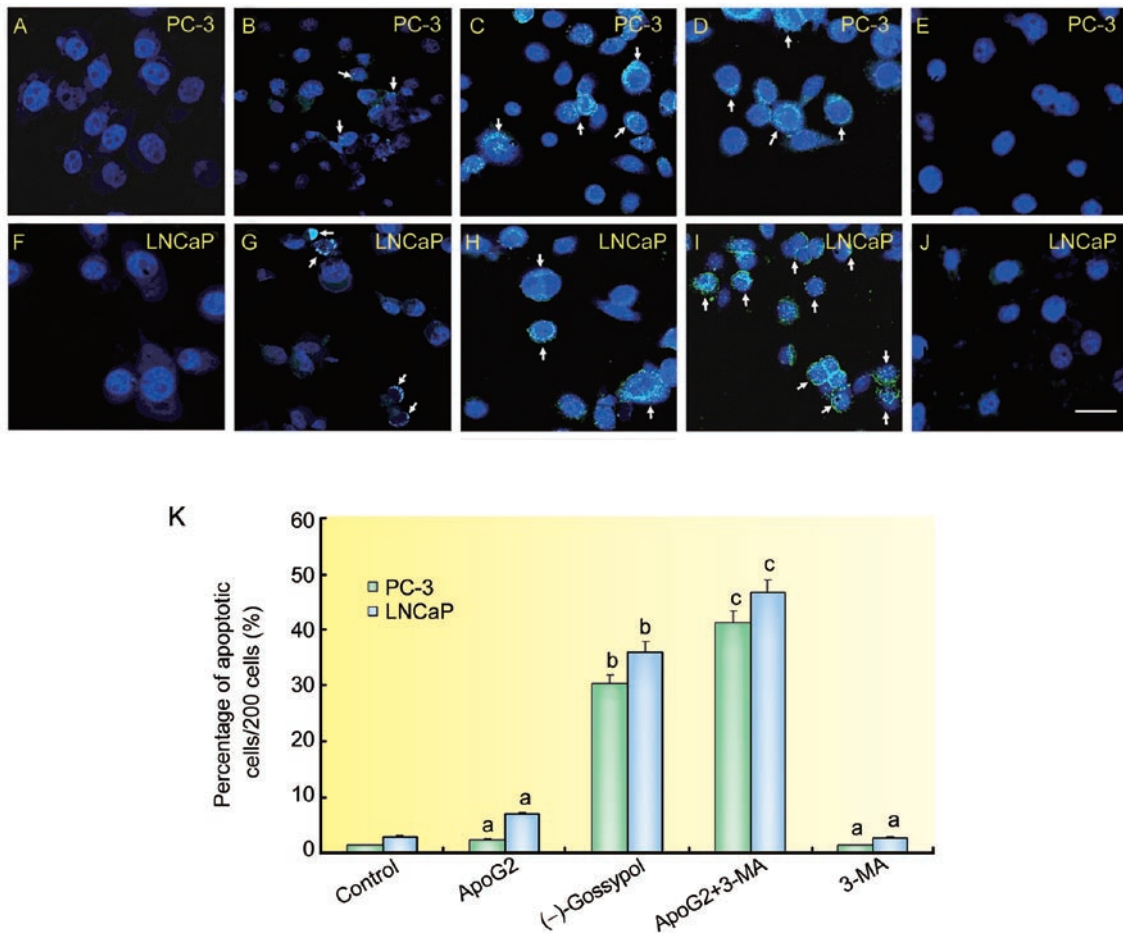
npg

Apogossypolone induces autophagy of prostate cancer cells *in vitro*
Xian-Qing Zhang *et al*.

704

Figure 3. Apoptotic cell death in PC-3 (A–E) and LNCaP (F–J) cells. The photomicrographs show controls (A, F), 10 mg L^{-1} ApoG2 (B, G), 10 mg L^{-1} (–)-gossypol (C, H), 10 mmol L^{-1} 3-MA+10 mg L^{-1} ApoG2 (D, I) and 3-MA (E, J) treated PC-3 and LNCaP cells. Bar = 20 μm. The TUNEL-positive nuclei are visualized in cyan, while Hochest33342-stained normal cell nuclei are visualized in blue. Cells in control exhibited only blue nuclei while the ApoG2 treatment produced a few TUNEL-positive nuclei (arrows). The histogram (K) represents the percentage (mean ± SD) of apoptotic nuclei (y-axis) per 200 cells for the conditions listed (x-axis). [a]$P > 0.05$, [b]$P < 0.01$, compared with control, [c]$P < 0.01$, compared with ApoG2.
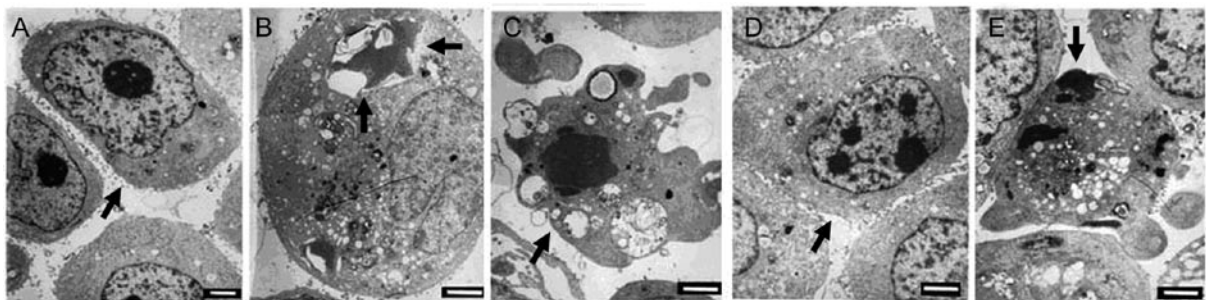

Figure 4. Ultrastructure of PC-3 cells treated with ApoG2 or (–)-gossypol. (A): DMSO-treated PC-3 cells at 24 h; (B): PC-3 cells treated with 10 mg L^{-1} ApoG2 at 24 h; (C): PC-3 cells treated with 10 mg L^{-1} ApoG2 at 72 h. (D): PC-3 cells treated with DMSO at 72 h; (E): PC-3 cells treated with 10 mg L^{-1} (–)-gossypol at 24 h. Arrows indicate normal cells (A and D), autophagosome (B), apoptosis cells (C and E); Bars = 1 μm.
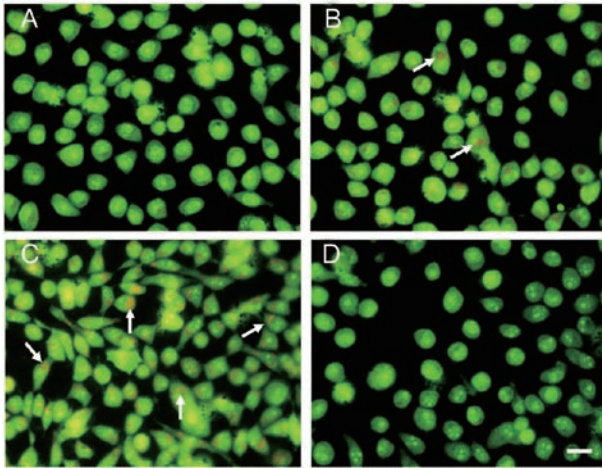
Figure 5. Indication of autophagy by acridine orange staining. (A): PC-3 cells treated with DMSO at 48 h; (B): PC-3 cells treated with 10 mg L^{-1} ApoG2 at 24 h; (C): PC-3 cells treated with 10 mg L^{-1} ApoG2 at 96 h; (D): PC-3 cells treated with 10 mg L^{-1} (–)-gossypol at 72 h. Arrows indicate acidic vesicular organelles. Bar = 20 μm.

Figure 6. ApoG2-induced autophagy in LNCaP cells. (A): LNCaP cells treated with 10 mg L^{-1} ApoG2 at 24 h with arrows to indicate the autophagosome-like structures; (B): LNCaP cells treated with 10 mg L^{-1} ApoG2 at 72 h with arrows to indicate the autophagosome-like structures; (C): LNCaP cells treated with DMSO at 72h. (D): Acridine orange staining of LNCaP cells treated with 10.0 mg L^{-1} ApoG2 at 24 h; (E): Acridine orange staining of LNCaP cells treated with DMSO at 24 h. (A)–(C): Bars = 1 μm. (D)–(E): Bars = 10 μm.

red fluorescence, again indicating a lack of AVOs (Figure 5D). These results provided further evidence to indicate that ApoG2 treatment caused autophagy in PC-3 cells.

3.4 ApoG2 also induced autophagy in LNCaP cells

Unlike PC-3 cells, the LNCaP cell line is androgen-responsive and contains the wild-type p53. Like PC-3 cells, however, treatment of LNCaP cells with 10 mg L^{-1} ApoG2 resulted in formation of autophagosome-like structures that were evident as early as 24 h (Figure 6A), and their number increased with exposure (Figure 6B). No such structures were observed in DMSO-treated PC-3 cells at 72 h (Figure 6C). In addition, ApoG2 treatment produced AVO in LNCaP cells, as revealed by acridine orange (Figure 6D). No AVO was detected in control (Figure 6E). Finally, similar to PC-3 cells, LNCaP cells with subdiploid DNA increased with ApoG2 treatment (data not shown) and cytoplasmic DNA fragmentation was significantly increased in the presence of 3-MA. Collectively, these results indicated that ApoG2-induced autophagy could be a common phenomenon and not restricted to any particular cell types.

4 Discussion

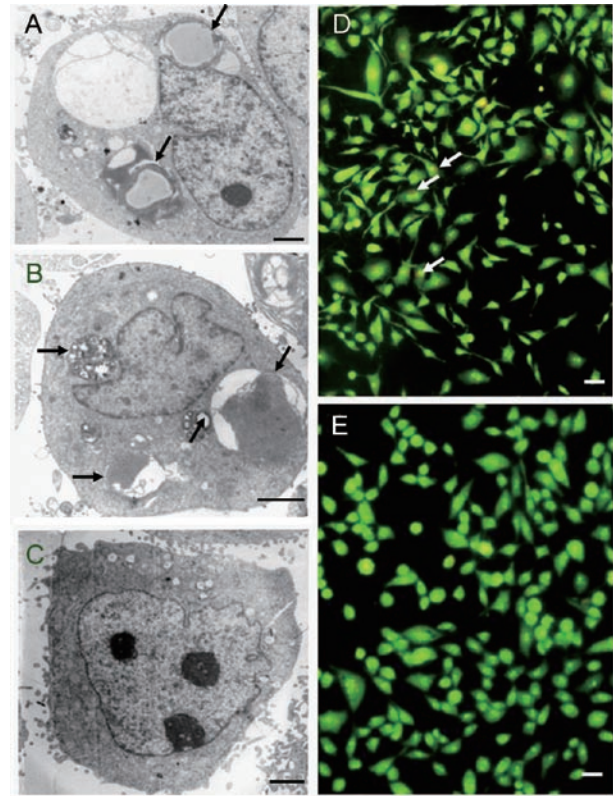The present study shows that (–)-gossypol and

ApoG2 inhibited growth of PC-3 and LNCaP cells in a time- and dose-dependent manner. The autophagy inhibitor 3-MA can enhance the growth-inhibitory effect of ApoG2 on both cell lines. The present study also provides experimental evidence to show activation of an autophagic program in human prostate cancer cells upon treatment with ApoG2, which is a highly promising nonpeptidic small-molecule inhibitor of Bcl-2. ApoG2-mediated autophagy in PC-3 and LNCaP cells is characterized by the appearance of membrane vacuoles containing remnants of mitochondria, and formation of AVOs. We also showed that the ApoG2-induced morphologic and biochemical changes-associated with autophagy preceded apoptosis. ApoG2-induced vacuoles and AVO were evident as early as 24 h

npg **Apogossypolone induces autophagy of prostate cancer cells *in vitro***
Xian-Qing Zhang *et al*.

706

after treatment and increased progressively with time, but the morphologic characteristics of apoptosis (e.g., chromatin condensation and DNA fragmentation) were not observed until 48 h later [43].

The autophagic pathway is a novel therapeutic target for cancer treatment [5–7, 44]. Such anticancer treatments would activate autophagy to kill cancer cells resistant to apoptosis. Paglin *et al*. [26] were the first to show the possibility of treating cancer cells by demonstrating that cancer cells respond to radiation with inhibition of autophagy. Autophagy inhibition enhances the anticancer effect of arsenic trioxide, hyperthermia [6], sulforaphane [45], and p53 or alkylating drugs [2]. These and our observations indicate that autophagy protects cancer cells from therapy-induced apoptosis and that autophagy inhibitors improve the efficacy of proapoptotic chemotherapeutic strategies. Autophagy is also commonly induced by hypoxia, and it represents the last nutritional intake mechanism for tumor cells to survive under low-nutrient conditions [6]. Thus, suppression of autophagy in combination with other treatments could accelerate tumor death [8, 46].

Cell death is subdivided into three categories: apoptosis (type I), autophagic cell death (type II) and necrosis (type III) [47]. Apoptosis is mediated by the activation of caspases and other factors released from the mitochondria. The molecular mechanism of apoptosis has been extensively studied, but that of autophagy is still obscure. The role of autophagy in cell death is controversial. Autophagy reportedly plays a protective role in allowing cells to survive during nutrient deprivation, and cells undergo apoptosis when autophagy is inhibited [48, 49]. However, the morphological features of autophagy have also been observed in dying cells in which caspases are suppressed or insufficiently activated [50, 51]. A more recent report demonstrated that oxidative stress-induced autophagic cell death is independent of apoptosis [52], indicating that autophagy and apoptosis may occur independently of each other.

Although the connection between autophagy and apoptotic cell death is not clear, autophagy seems to promote apoptosis in some systems. For example, the formation of autophagosomes has been shown to be associated with TNF-α-induced apoptosis in human T lymphoblastic leukemia cells. In this model, inhibition of autophagy by 3-MA also inhibits DNA fragmentation [53]. More recently, Li *et al*. [54] have shown that 5-FU-induced apoptosis in colon cancer cells can be enhanced by 3-MA. Ding *et al*. [55] proved that inhibition by 3-MA enhanced apoptotic cell death induced by MG132 (a commonly used proteasome inhibitor) in not only Bax-positive HCT116 cells but also Bax-negative cells [55]. Shingu *et al*. [56] also found that the therapeutic efficacy of imatinib for malignant glioma might be augmented by 3-MA at a late stage, and that appropriate modulation of autophagy might sensitize tumor cells to anticancer therapy. Herman-Antosiewicz *et al*. [45] reported that autophagy represented a defense mechanism against sulforaphane-induced apoptosis in human prostate cancer cells. This conclusion was based on the observations that sulforaphane-induced release of cytochrome *c* and apoptosis were significantly increased in the presence of 3-MA.

Apoptosis induction by certain sulforaphane analogs (e.g., phenethyl isothiocyanate) is regulated by p53 in some cells [57, 58]. For instance, mouse embryonic fibroblasts lacking p53 are resistant to phenethyl isothiocyanate-induced apoptosis compared to fibroblasts with p53 [58]. The present study suggests that p53 may not be required for ApoG2-induced autophagy or apoptosis because both PC-3 and LNCaP cells are sensitive to ApoG2-induced autophagy and apoptosis.

Formation of autophagosomes is a complex process regulated by multiple molecules [59, 60]. A cup-shaped isolation membrane first forms around cytosolic components and it eventually fuses into a double membrane-bound vesicle. This autophagosome undergoes several microtubule-dependent maturation events, including fusion with endosomes and multilamellar vesicles, before fusion with lysosomes [61, 62].

In conclusion, our observations indicate that apoptosis induction by ApoG2 in PC-3 and LNCaP human prostate cancer cells can be enhanced by inhibition of autophagy. This is the first published report to document activation of an autophagic program in the context of apoptosis by ApoG2. It is reasonable to speculate that autophagy inhibition may help to enhance the chemopreventive/therapeutic activity of ApoG2. We have shown that ApoG2 could significantly increase the life span of PC-3 and LNCaP prostate cancer-bearing nude mice. We also found that the hepatotoxicity and gastrointestinal toxicity of ApoG2 was lower than that of (–)-gossypol (data not shown). Therefore, ApoG2 could potentially be a more effective drug in the prostate cancer therapy.

Apogossypolone induces autophagy of prostate cancer cells *in vitro*
Xian-Qing Zhang *et al*.

npg

707

5 Conflict of interest

The authors declare no potential conflicts of interest.

Acknowledgement

References

1   Mizushima N, Levine B, Cuervo AM, Klionsky DJ. Autophagy fights disease through cellular self-digestion. Nature 2008; 451: 1069–75.

2   Amaravadi RK, Thompson CB. The roles of therapy-induced autophagy and necrosis in cancer treatment. Clin Cancer Res 2007; 13: 7271–9.

3   Kisen GO, Tessitore L, Costelli P, Gordon PB, Schwarze PE, *et al*. Reduced autophagic activity in primary rat hepatocellular carcinoma and ascites hepatoma cells. Carcinogenesis 1993; 14: 2501–5.

4   Canuto RA, Tessitore L, Muzio G, Autelli R, Baccino FM. Tissue protein turnover during liver carcinogenesis. Carcinogenesis 1993; 14: 2581–7.

5   Levine B, Kroemer G. Autophagy in the pathogenesis of disease. Cell 2008; 132: 27–42.

6   Kondo Y, Kanzawa T, Sawaya R, Kondo S. The role of autophagy in cancer development and response to therapy. Nat Rev Cancer 2005; 5: 726–34.

7   Levine B. Cell biology: autophagy and cancer. Nature 2007; 446: 745–7.

8   Mathew R, Karantza-Wadsworth V, White E. Role of autophagy in cancer. Nat Rev Cancer 2007; 7: 961–7.

9   Longo L, Platini F, Scardino A, Alabiso O, Vasapollo G, *et al*. Autophagy inhibition enhances anthocyanin-induced apoptosis in hepatocellular carcinoma. Mol Cancer Ther 2008; 7: 2476–85.

10 Diaz M, Patterson SG. Management of androgen-independent prostate cancer. Cancer Control 2004; 11: 364–73.

11 Gioeli D. Signal transduction in prostate cancer progression. Clin Sci (Lond) 2005; 108: 293–308.

12 Jemal A, Murray T, Ward E, Samuels A, Tiwari RC, *et al*. Cancer statistics, 2005. CA Cancer J Clin 2005; 55: 10–30.

13 Coutinho EM. Gossypol: a contraceptive for men. Contraception 2002; 65: 259–63.

14 Cui GH, Xu ZL, Yang ZJ, Xu YY, Xue SP. A combined regimen of gossypol plus methyltestosterone and ethinylestradiol as a contraceptive induces germ cell apoptosis and expression of its related genes in rats. Contraception 2004; 70: 335–42.

15 Balci A, Sahin FI, Ekmekci A. Gossypol induced apoptosis in the human promyelocytic leukemia cell line HL 60. Tohoku J Exp Med 1999; 189: 51–7.

16 Zhang M, Liu H, Guo R, Ling Y, Wu X, *et al*. Molecular

mechanism of gossypol-induced cell growth inhibition and cell death of HT-29 human colon carcinoma cells. Biochem Pharmacol 2003; 66: 93–103.

17 Rekha GK, Sladek NE. Inhibition of human class 3 aldehyde dehydrogenase, and sensitization of tumor cells that express significant amounts of this enzyme to oxazaphosphorines, by the naturally occurring compound gossypol. Adv Exp Med Biol 1997; 414: 133–46.

18 Hu YF, Chang CJ, Brueggemeier RW, Lin YC. Gossypol inhibits basal and estrogen-stimulated DNA synthesis in human breast carcinoma cells. Life Sci 1993; 53: PL433–8.

19 Jiang J, Kulp SK, Sugimoto Y, Liu S, Lin YC. The effects of gossypol on the invasiveness of MAT-LyLu cells and MAT-LyLu cells from the metastasized lungs of MAT-LyLu-bearing Copenhagen rats. Anticancer Res 2000; 20: 4591–7.

20 Jiang J, Sugimoto Y, Liu S, Chang HL, Park KY, *et al*. The inhibitory effects of gossypol on human prostate cancer cells-PC3 are associated with transforming growth factor beta1 (TGFbeta1) signal transduction pathway. Anticancer Res 2004; 24: 91–100.

21 Xu L, Yang D, Wang S, Tang W, Liu M, *et al*. (–)-Gossypol enhances response to radiation therapy and results in tumor regression of human prostate cancer. Mol Cancer Ther 2005; 4: 197–205.

22 Zhang M, Liu H, Tian Z, Griffith BN, Ji M, Li QQ. Gossypol induces apoptosis in human PC-3 prostate cancer cells by modulating caspase-dependent and caspase-independent cell death pathways. Life Sci 2007; 80: 767–74.

23 Arnold AA, Aboukameel A, Chen J, Yang D, Wang S, *et al*. Preclinical studies of Apogossypolone: a new nonpeptidic pan small-molecule inhibitor of Bcl-2, Bcl-XL and Mcl-1 proteins in Follicular Small Cleaved Cell Lymphoma model. Mol Cancer 2008; 7: 20.

24 Sun J, Li ZM, Hu ZY, Lin XB, Zhou NN, *et al*. ApoG2 inhibits antiapoptotic Bcl-2 family proteins and induces mitochondria-dependent apoptosis in human lymphoma U937 cells. Anticancer Drugs 2008; 19: 967–74.

25 Romijn JC, Verkoelen CF, Schroeder FH. Application of the MTT assay to human prostate cancer cell lines *in vitro*: establishment of test conditions and assessment of hormone-stimulated growth and drug-induced cytostatic and cytotoxic effects. Prostate 1988; 12: 99–110.

26 Paglin S, Hollister T, Delohery T, Hackett N, McMahill M, *et al*. A novel response of cancer cells to radiation involves autophagy and formation of acidic vesicles. Cancer Res 2001; 61: 439–44.

27 Traganos F, Darzynkiewicz Z. Lysosomal proton pump activity: supravital cell staining with acridine orange differentiates leukocyte subpopulations. Methods Cell Biol 1994; 41: 185–94.

28 Stankiewicz M, Jonas W, Hadas E, Cabaj W, Douch PG. Supravital staining of eosinophils. Int J Parasitol 1996; 26: 445–6.

29 Liang XH, Kleeman LK, Jiang HH, Gordon G, Goldman JE, *et al*. Protection against fatal Sindbis virus encephalitis by beclin, a novel Bcl-2-interacting protein. J Virol 1998; 72: 8586–96.

30 Liang XH, Jackson S, Seaman M, Brown K, Kempkes B,

Apogossypolone induces autophagy of prostate cancer cells *in vitro*
Xian-Qing Zhang *et al*.

708

et al. Induction of autophagy and inhibition of tumorigenesis by beclin 1. Nature 1999; 402: 672–6.

31 Qu X, Yu J, Bhagat G, Furuya N, Hibshoosh H, *et al*. Promotion of tumorigenesis by heterozygous disruption of the beclin 1 autophagy gene. J Clin Invest 2003; 112: 1809–20.

32 Yue Z, Jin S, Yang C, Levine AJ, Heintz N. Beclin 1, an autophagy gene essential for early embryonic development, is a haploinsufficient tumor suppressor. Proc Natl Acad Sci USA 2003; 100: 15077–82.

33 Yue Z, Horton A, Bravin M, DeJager PL, Selimi F, *et al*. A novel protein complex linking the delta 2 glutamate receptor and autophagy: implications for neurodegeneration in lurcher mice. Neuron 2002; 35: 921–33.

34 Cao Y, Klionsky DJ. Physiological functions of Atg6/Beclin 1: a unique autophagy-related protein. Cell Res 2007; 17: 839–49.

35 Zeng X, Overmeyer JH, Maltese WA. Functional specificity of the mammalian Beclin-Vps34 PI 3-kinase complex in macroautophagy versus endocytosis and lysosomal enzyme trafficking. J Cell Sci 2006; 119: 259–70.

36 Luo S, Rubinsztein DC. Apoptosis blocks Beclin 1-dependent autophagosome synthesis: an effect rescued by Bcl-xL. Cell Death Differ; 17: 268–77.

37 Pattingre S, Tassa A, Qu X, Garuti R, Liang XH,*et al*. Bcl-2 antiapoptotic proteins inhibit Beclin 1-dependent autophagy. Cell 2005; 122: 927–39.

38 Kim YA, Xiao D, Xiao H, Powolny AA, Lew KL, *et al*. Mitochondria-mediated apoptosis by diallyl trisulfide in human prostate cancer cells is associated with generation of reactive oxygen species and regulated by Bax/Bak. Mol Cancer Ther 2007; 6: 1599–609.

39 Shih CM, Wu JS, Ko WC, Wang LF, Wei YH, *et al*. Mitochondria-mediated caspase-independent apoptosis induced by cadmium in normal human lung cells. J Cell Biochem 2003; 89: 335–47.

40 Gavrieli Y, Sherman Y, Ben-Sasson SA. Identification of programmed cell death in situ via specific labeling of nuclear DNA fragmentation. J Cell Biol 1992; 119: 493–501.

41 Klionsky DJ, Abeliovich H, Agostinis P, Agrawal DK, Aliev G, *et al*. Guidelines for the use and interpretation of assays for monitoring autophagy in higher eukaryotes. Autophagy 2008; 4: 151–75.

42 Daido S, Kanzawa T, Yamamoto A, Takeuchi H, Kondo Y, Kondo S. Pivotal role of the cell death factor BNIP3 in ceramide-induced autophagic cell death in malignant glioma cells. Cancer Res 2004; 64: 4286–93.

43 Singh SV, Srivastava SK, Choi S, Lew KL, Antosiewicz J, *et al*. Sulforaphane-induced cell death in human prostate cancer cells is initiated by reactive oxygen species. J Biol Chem 2005; 280: 19911–24.

44 Rubinsztein DC, Gestwicki JE, Murphy LO, Klionsky DJ. Potential therapeutic applications of autophagy. Nat Rev Drug Discov 2007; 6: 304–12.

45 Herman-Antosiewicz A, Johnson DE, Singh SV. Sulforaphane causes autophagy to inhibit release of cytochrome C and apoptosis in human prostate cancer cells. Cancer Res 2006; 66: 5828–35.

46 Lum JJ, DeBerardinis RJ, Thompson CB. Autophagy in metazoans: cell survival in the land of plenty. Nat Rev Mol Cell Biol 2005; 6: 439–48.

47 Lockshin RA, Zakeri Z. Apoptosis, autophagy, and more. Int J Biochem Cell Biol 2004; 36: 2405–19.

48 Boya P, Gonzalez-Polo RA, Casares N, Perfettini JL, Dessen P, *et al*. Inhibition of macroautophagy triggers apoptosis. Mol Cell Biol 2005; 25: 1025–40.

49 Lum JJ, Bauer DE, Kong M, Harris MH, Li C, *et al*. Growth factor regulation of autophagy and cell survival in the absence of apoptosis. Cell 2005; 120: 237–48.

50 Shimizu S, Kanaseki T, Mizushima N, Mizuta T, Arakawa-Kobayashi S, *et al*. Role of Bcl-2 family proteins in a non-apoptotic programmed cell death dependent on autophagy genes. Nat Cell Biol 2004; 6: 1221–8.

51 Yu L, Alva A, Su H, Dutt P, Freundt E, *et al*. Regulation of an ATG7-beclin 1 program of autophagic cell death by caspase-8. Science 2004; 304: 1500–2.

52 Chen Y, McMillan-Ward E, Kong J, Israels SJ, Gibson SB. Oxidative stress induces autophagic cell death independent of apoptosis in transformed and cancer cells. Cell Death Differ 2008; 15: 171–82.

53 Jia L, Dourmashkin RR, Allen PD, Gray AB, Newland AC, *et al*. Inhibition of autophagy abrogates tumour necrosis factor alpha induced apoptosis in human T-lymphoblastic leukaemic cells. Br J Haematol 1997; 98: 673–85.

54 Li J, Hou N, Faried A, Tsutsumi S, Takeuchi T, *et al*. Inhibition of autophagy by 3-MA enhances the effect of 5-FU-induced apoptosis in colon cancer cells. Ann Surg Oncol 2009; 16: 761–71.

55 Ding WX, Ni HM, Chen X, Yu J, Zhang L, *et al*. A coordinated action of Bax, PUMA, and p53 promotes MG132-induced mitochondria activation and apoptosis in colon cancer cells. Mol Cancer Ther 2007; 6: 1062–9.

56 Shingu T, Fujiwara K, Bogler O, Akiyama Y, Moritake K, *et al*. Inhibition of autophagy at a late stage enhances imatinib-induced cytotoxicity in human malignant glioma cells. Int J Cancer 2009; 124: 1060–71.

57 Fimognari C, Nusse M, Cesari R, Iori R, Cantelli-Forti G, *et al*. Growth inhibition, cell-cycle arrest and apoptosis in human T-cell leukemia by the isothiocyanate sulforaphane. Carcinogenesis 2002; 23: 581–6.

58 Marionnet C, Armier J, Sarasin A, Stary A. Cyclobutane pyrimidine dimers are the main mutagenic DNA photoproducts in DNA repair-deficient trichothiodystrophy cells. Cancer Res 1998; 58: 102–8.

59 Fallow GD, Singh J. The prevalence, type and severity of cardiovascular disease in diabetic and non-diabetic patients: a matched-paired retrospective analysis using coronary angiography as the diagnostic tool. Mol Cell Biochem 2004; 261: 263–9.

60 Klionsky DJ. The molecular machinery of autophagy: unanswered questions. J Cell Sci 2005; 118: 7–18.

61 Berg TO, Fengsrud M, Stromhaug PE, Berg T, Seglen PO. Isolation and characterization of rat liver amphisomes. Evidence for fusion of autophagosomes with both early and late endosomes. J Biol Chem 1998; 273: 21883–92.

62 Eskelinen EL. Maturation of autophagic vacuoles in mammalian cells. Autophagy 2005; 1: 1–10.